This Page Is Inserted by IFW Operations
and is not a part of the Official Record

BEST AVAILABLE IMAGES

Defective images within this document are accurate representations of the original documents submitted by the applicant.

Defects in the images may include (but are not limited to):

- BLACK BORDERS

- TEXT CUT OFF AT TOP, BOTTOM OR SIDES

- FADED TEXT

- ILLEGIBLE TEXT

- SKEWED/SLANTED IMAGES

- COLORED PHOTOS

- BLACK OR VERY BLACK AND WHITE DARK PHOTOS

- GRAY SCALE DOCUMENTS

IMAGES ARE BEST AVAILABLE COPY.

As rescanning documents *will not* correct images, please do not report the images to the Image Problem Mailbox.

Rapid Solidification of Ceramics
A Technology Assessment

by

M. C. Brockway and R. R. Wills
Battelle's Columbus Laboratories
Columbus, Ohio 43201

TABLE OF CONTENTS

TABLE OF CONTENTS
(Continued)

INTRODUCTION

A recent state-of-the-art review of rapid solidification technology (RST)[1] as applied to metals indicates that an exciting "new metallurgy" is forming around the concept of rapid solidification. This report examines the status and potential of RST as applied to ceramics.

The basic effect of applying rapid cooling to ceramics is analogous to that for metals. It suppresses diffusion within the material and thus inhibits the attainment of equilibrium crystal phases and microstructures which are characteristic of "slowly" cooled materials. Thus, the expected effects (benefits) from rapid solidification (RS) of ceramics are also similar to metals, namely:

(1) Grain size decrease with increasing solidification rate

(2) Increased chemical homogeneity (optimization) with increasing solidification rate

(3) Extension of solid solubility with increasing solidification rate

(4) Metastable crystal structures, some previously unreported

(5) "Complete" suppression of crystallization to produce noncrystalline, amorphous or vitreous (glassy) ceramics.

In the research to date on RS ceramics, attention has focused on effects (3) through (5) above.

The primary objectives of this report are to:

● Provide a comprehensive summary of ceramic RST research to date

● Summarize reported properties of rapidly solidified ceramics and potential areas of utility

● Identify and discuss the factors retarding development or application of RS ceramics

● Present recommendations for accelerating the development and application of RS ceramics.

It has taken several decades from the initial research on rapidly solidified metals to develop the emerging commercial processes of today. By utilizing and building on the rapid solidification technology of metals, it should be possible to shorten the time for realizing commercial RS processing of ceramics.

SUMMARY

The application of rapid solidification technology to ceramics is in the early exploratory research stage. Fairly extensive laboratory studies have demonstrated unique or potentially valuable properties for RS ceramics including: ionic conductivities many orders of magnitude higher than for polycrystalline forms of the same compositions, temperature dependent high dielectric constants, electrochromism, pyroelectric characteristics, semiconductivities, magnetic characteristics, long wavelength IR transmission, and anisotropy. No known efforts are currently in progress to commercialize any of these materials.

Except for a few studies on sulfates and fluorides, RS ceramic studies have been limited to oxide systems. The results of these studies indicate that a very large number of ceramic compositions can be produced in noncrystalline or glass form using cooling rates of $\geq 10^6$ K/sec.

The potential of rapid solidification processing to produce ceramics with valuable new property characteristics or new levels of performance appears to justify a major research commitment. It is recommended that research emphasize the development of process technology capable of:

- Producing quenched noncrystalline and glass powders in commercial quantities
- Producing continuous fiber, foil, or strip and powders
- Consolidating RS powders into useful forms while retaining the metastable powder microstructures without introducing competing or degrading side effects
- Applying thin noncrystalline or glass coatings.

It is also recommended that RS research be conducted to explore the mechanical properties which might be achieved via RS materials, and to continue the general laboratory studies on RS ceramic materials.

STATUS OF RAPIDLY SOLIDIFIED CERAMICS TECHNOLOGY

This technology assessment is divided into three parts for discussion: (1) the processes, techniques, and equipment developed for rapid solidification, (2) the RS ceramic materials produced, and (3) the demonstrated properties of these materials.

RAPID SOLIDIFICATION PROCESSES, TECHNIQUES, AND EQUIPMENT

Before discussing rapid solidification processes and techniques, it is helpful to define the range of cooling rates involved. Published research on rapid solidification of ceramics has spanned the cooling range from $\sim 10^3$ to $\sim 10^9$ K/sec. A qualitative sense of these rates may be obtained from the following examples:

o A small pellet dropped into mercury cools at a rate of $\sim 10^2$ to 10^3 K/sec

o A small droplet of melt impacted and spread into a thin film on a metal quench surface (splat cooling) cools at $\sim 10^5$ to 10^7 K/sec.

Rapid solidification processes involve two operations: (1) the generation of a suitable melt and (2) the rapid solidification (cooling) of the melt. A discussion of several reported laboratory techniques for rapidly cooling ceramics follows.

Laser Spin Melt With Free Fall Cooling

This technique reported by Topol[2] is one of the simplest techniques for rapid solidification. A laser beam is directed onto the end of a rapidly rotating, horizontally oriented ceramic rod. As the end of the rod melts, molten droplets spin off and cool by free fall through the air. Quenched spherules were produced in sizes ranging from about 100 to 800 μm depending on the ceramic material, speed of rotation, and laser beam power density. Although the process is simple to implement, it provides relatively low cooling rates of about 10^3 to 10^4 K/sec and probably poor process control in terms of melt temperature and quench rates of individual spherules.

Taylor Wire Technique

This process is basically a duplex fiber drawing process in which the material of prime interest is drawn as the core of a glass-clad fiber. It has been primarily utilized to form metallic microfilaments as the core component. However, Pardoe[3] has shown that the

process may be utilized to form rapidly solidified ceramics as the core material. Figure 1 illustrates the process with metal as the core material.

The Taylor process is capable of providing cooling rates in the range of about 10^3 to 10^5 K/sec. The major disadvantage is the high probability of chemical reaction between the core and sheath materials leading to contamination of the core.

Plasmatron Technique

Revcolevschi[4] has reported the applicability of a plasmatron to produce fine quenched powders. Fine powder is injected into a plasma and blown onto a rotating metallic disk (Figure 2). The plasmatron is operated under 20 V and 260 A at gas flow rates of 30 liters/min; the molten droplets impinge on a brass disk 7.9 in. (20 cm) in diameter and 0.28 in. (7 mm) thick, rotating at 60 rpm. The lower part of the disk is immersed in distilled water to a depth of 3.1 in. (8 cm). The quenched material is then collected in the water. The powder

FIGURE 1. SCHEMATIC REPRESENTATION OF THE TAYLOR WIRE PROCESS UTILIZING A DOUBLE BUSHING TO DRAW A CLAD TWO-COMPONENT WIRE[3]

FIGURE 2. PLASMATRON QUENCHING APPARATUS [4]

distributor is made of a cylindrical reservoir, 0.79 in. (20 mm) in diameter, in which the oxide is placed on a fritted-glass pellet welded to the cylinder. Argon flow rates ranging from 0 to 15 liters/hr facilitate the fluidization of the powder and its flow through the plasmatron. The plasma nozzle is placed at a distance of 0.6 in. (15 mm) from the disk. The temperatures attained in the plasma allow quenching from melts above 5432 F (3000 C). The quenched samples are in the form of a fine powder and the cooling rate is estimated at about 10^5 K/sec.

Hammer and Anvil Technique

This technique smashes a melt between the surfaces of a metal hammer and anvil so as to produce a thin melt layer in close contact with the metal for rapid quenching. Three experimental devices employing this technique are shown in Figures 3, 4, and 5. The first scheme (Figure 3) employs a laser to melt the tip of a ceramic rod from which a droplet falls between the hammer and anvil.[20] A timing device releases the hammer in order to impact and quench the falling droplet. A deficiency of this device is the cooling rate of the droplet during the time of fall. Quench rates up to $\approx 10^5$ K/sec are reported possible for metal samples quenched by this technique. Ceramic quench rates might be somewhat lower.

FIGURE 3. HAMMER AND ANVIL DEVICE FOR QUENCHING LASER MELT SAMPLES[20]

Figure 4 illustrates a hammer and anvil quench device reported by Shishido.[5] A primary advantage of this device is that the melt is formed in situ on the anvil, thus eliminating cooling during free fall as in the preceding device. Quench rates estimated for oxide samples using this device were ≈8×10^7 K/sec.

Revcolevschi[4] reports a third variation of the hammer and anvil technique in which solar energy is utilized to melt the ceramic sample. This device is illustrated in Figure 5. Attainable cooling rates for this device were estimated as 10^4 to 10^5 K/sec.

Arc melting has also been utilized in conjunction with hammer and anvil quenching. A device utilized by Ohring[6] is illustrated in Figure 6. In this apparatus the samples are placed on a lapped planar depression which serves as the anvil. An aluminum hammer is positioned above the sample. When the sample is arc melted the hammer is released to impact, spread, and quench the melt. The estimated quench rate was ≈10^5 K/sec.

Single Roller Quenching

Suzuki[7] reports the use of a single roller quench technique. The procedure is to melt the ceramic in a platinum tube 4 in. (10 cm) long by 0.2 in. (5 mm) inner diameter. (Presumably the melting is by induction heating.) The melt is pressurized to force it through an 0.012 in. (0.3 mm) orifice in the tip (bottom) of the tube and to feed the liquid stream onto

FIGURE 4. RAPID QUENCHING APPARATUS INCORPORATING A LASER BEAM(5)

the surface of a 7.9 in. (20 cm) diameter stainless steel roller rotating at speeds between 1,500 and 6,000 rpm. Typical quenched sample films were 0.8 in. (2 cm) long, 0.016 to 0.024 in. (0.4 to 0.6 mm) wide, and 15 μm thick. It should be noted the quench technique requires that the ceramic melt wet the metal roller in order for it to spread and form a film for quenching. Figure 7 schematically illustrates this process. Shibata(8) also utilized the single roller technique and estimated quench rates of about 10^5 K/sec.

Centrifugal Quenching

This technique feeds a liquid (melt) stream onto the inner surface of a rotating metal quench drum. The technique has been reported by Suzuki(9) who utilized an aluminum drum with a 5.9 in. (15 cm) inner diameter rotating at 1,000 rpm into which he injected a thin stream of melt. He produced quenched ribbons about 0.08 in. (2 mm) wide by 3.94 in. (10 cm)

FIGURE 5. HAMMER AND ANVIL DEVICE ASSOCIATED WITH A SOLAR FURNACE[4]

long ranging in thickness from 1 to 40 μm. No estimate of quench rate was made. Figure 8 schematically illustrates this centrifugal quenching method.

Air Gun Splat Cooling

Gun splat cooling utilizes the high velocity shock wave of an air gun to drive droplets of melt onto a metal quench surface. As the droplets impact the surface they spread or "splat" and quench. This was the earliest technique applied to ceramics and there are many variations.

In the pioneering RS work on ceramic materials Sarjeant and Roy[10] used a variation of the apparatus employed earlier by Duwez and Willens[11] for quenching metals. The equipment of Sarjeant and Roy, shown in Figure 9, consisted essentially of two parts, a strip heater and an air-powered shock tube. The strip furnace consisted of a thin strip or wire of refractory metal connected to a power source. A few milligrams of the ceramic oxide under study were melted in a V-notch in the strip and maintained at about 100 K above the liquidus. The air gun was then fired to drive the melt from the strip onto the substrate. Estimated attainable cooling rates for splat cooling are above 10^5 to 10^7 K/sec.

Jantzen[12] utilized laser melting in combination with a variation of the Duwez splat-quench technique. The apparatus is illustrated in Figure 10. A molten drop of melt was formed on the bottom of a ceramic rod. An air gun was employed to blast the drop off the rod

Translatory (Wilson) Seals

Water Inlet

Water Inlet

Water Cooled Coaxial Copper Rod
(Electrically Connected to Welding Machine)

Vacuum Hose

Inert Tungsten
Electrode

Copper
Hearth

Argon Gas Inlet

To Vacuum

Nut

Arrow Holder

Springs
Arrow

Ball Bushing Bearing

Hammer Assembly
Sample Melted on Anvil

Glass Ring

Water Inlet

FIGURE 6. ARC MELT HAMMER AND ANVIL QUENCH DEVICE(6)

and onto a copper substrate for quenching. Estimated attainable quench rates for this apparatus were up to about 10^7 K/sec.

Revcolevschi[4] describes another variation of the gun splat technique which employs an image furnace floating zone for the melt. This apparatus, shown schematically in Figure 11, permits operating up to 4170 F (2300 C). Estimated attainable quench rates are about 10^6 K/sec.

Twin Roller Quenching

This technique has been utilized extensively for many of the better documented RS studies on ceramics. The primary variation of the technique among researchers has been the method of forming and delivering the melt.

FIGURE 7. SCHEMATIC OF THE SINGLE ROLLER TECHNIQUE[7]

FIGURE 8. SCHEMATIC OF THE CENTRIFUGAL
QUENCHING TECHNIQUE[9]

Valve

To Compressed
Air Source

Cellophane Diaphragm

Threaded
Coupling

O-Ring
Gasket

Threaded
Flange

Platinum Nozzle

Strip Heater

Variac

110 V

Substrate

6.5 V Transformer

FIGURE 9. SCHEMATIC OF THE SPLAT-QUENCH APPARATUS(10)

Curved Copper
Substrate

Lens

Specimen

CO_2 Laser

Platinum
Nozzle

Duwez-Type
Splat Gun

Toggle
Switch

To High
Pressure
Tank

FIGURE 10. LASER MELT QUENCH APPARATUS USING DUWEZ-TYPE SPLAT-GUN TECHNIQUE(12)

Gun   Liquid

A

B

High Pressure Gas   Water Cooled Substrate

FIGURE 11. SPLAT COOLING ADAPTED TO AN IMAGE FURNACE FLOATING ZONE[4]

The initial use of twin rollers by Chen and Miller[13] merely allowed the melt to drop between two counter rotating rollers as illustrated in Figure 12. The melt solidifies as it passes through the roller to form flake or "foil" geometries for quenched ceramics or strip for ductile metals. Attainable cooling rates were estimated to be about 10^5 K/sec.

Tatsumisago[14] has utilized a thermal image furnace for sample melting plus an after heater to better control the melt droplet temperature as it drops to contact the twin rollers. This is illustrated in Figure 13. Attainable cooling rates were estimated to be as high as $\approx 10^9$ K/sec.

Suzuki and Anthony[15] have utilized plasma torch melting and projection in conjunction with twin roller quenching (Figure 14). A ceramic rod specimen was inserted into the plasma leading to melting and injection between the rollers. The technique permitted melting and quenching compositions with melting points up to 4080 F (2250 C). Attainable quench rate was estimated at 10^5 K/sec.

The most extensively utilized and possibly the most controllable twin roller equipment is that reported by Nassau et al. of Bell Laboratories.[16] As shown in Figure 15, this design utilizes an inductively heated crucible melt which may be pressurized to eject it between the rollers. This basic design has been utilized by Bell Labs to rapidly quench a wide range of

Heater

Rollers

p

p

Quenched
Strip

FIGURE 12. TWIN ROLLER APPARATUS(13)

Ellipsoidal
Reflector

Quartz Tube

Sample

Screen

After Heater

Halogen Lamp

Twin Roller

FIGURE 13. TWIN ROLLER QUENCHING APPARATUS(14)

FIGURE 14. SCHEMATIC OF PLASMA MELT TWIN ROLLER QUENCH APPARATUS[15]

oxide melts and a lesser number of sulfate melts. Attainable quench rates were estimated as $\approx 10^7$ K/sec.

Roller-Plate Quench

Torii[17] reported an interesting variation of the twin roller quench. This is shown schematically in Figure 16. Instead of injecting melt between steel rollers, it is injected between two metal "plates" (strips) which are drawn between rubber rollers. This arrangement provides planar contact instead of the line contact of steel rollers (presumably providing for a better quench). No estimate of quench rate was made.

FIGURE 15. TWIN ROLLER QUENCH APPARATUS(17)

Pendant Drop Melt Extraction

This technique, as illustrated in Figure 17, brings a rotating wheel into contact with a molten drop on the tip of a ceramic rod. In unpublished studies at Battelle-Columbus, the technique has been implemented by employing a laser to form the molten pendant drop on the feed rod. It has been possible to extract and form quenched products in the form of particles, fibers, or micro-foils. Examples of these products are discussed in the subsequent section on RS ceramic materials. Accurate estimates of the attained quench rates were not made, but micro-foils exhibiting areas of noncrystallinity (based on diffraction) suggest quench rates of $\approx 10^6$ K/sec.

FIGURE 16. SCHEMATIC OF ROLLER-PLATE QUENCH APPARATUS[17]

Evaporative Decomposition of Solutions (EDS)

This process uses a two-fluid atomizer to inject salt solutions or suspensions into a vertical furnace hot zone as a mist (Figure 18). Solvent removal and decomposition of the residual salt particles are accomplished in a few seconds to yield highly reactive and homogeneous crystalline and noncrystalline fine oxide powders. The minimum "effective quench rate" has been estimated to be 6×10^7 K/sec. This "effective quench rate" means that the EDS[18] process has been able to produce metastable forms of ceramics which have required this quench rate when produced by rapid solidification.

Because this EDS process does not involve rapid solidification it might technically be considered inappropriate to include it in this report. However, since the process is capable of producing noncrystalline or metastable ceramic powders, it is an alternate route to RS production of powders. EDS powders could be utilized assuming that consolidation processes can be developed to process such powders into useful products while retaining the metastable or noncrystalline microstructure.

Top View of Wheel

90°

↻

Rotatable and Translatable Ceramic Rod

Laser Beam

Extraction Wheel

FIGURE 17. SCHEMATIC OF THE EXPERIMENTAL SET-UP FOR PENDANT DROP MELT EXTRACTION EXPERIMENTS

Summary Comments on RS Processes

Based upon published literature it can be concluded that only laboratory-scale processes have been developed for rapid solidification of ceramic materials. Even on a laboratory scale, none of the processes are capable of producing continuous forms such as ribbons or foils. Research to date has focused on exploring the properties of RS ceramics rather than process development.

FIGURE 18. SCHEMATIC OF A LABORATORY VERSION OF THE EDS PROCESS[18]

RAPIDLY SOLIDIFIED CERAMIC MATERIALS

The rapid solidification processes discussed have been applied to a large number of oxide compositions, a small number of sulfate compositions, and a very few halide compositions.

A comprehensive listing of the research studies performed on rapidly solidified ceramics is provided in the Appendix, Tables A-1 through A-4. These tables summarize the compositions studied, the RS techniques employed, the approximate quench rates, the physical geometry of quenched products, the metastable forms achieved, and the analytical verification techniques applied to the metastable forms. The properties demonstrated for quenched products are summarized in a subsequent section.

Before discussing the tables it is desirable to clarify the meaning of the commonly used terms noncrystalline and glass. The designation noncrystalline is applied to quenched products which exhibit short range order only, i.e., those that show only a broad diffuse scattering to X-rays indicating no order beyond about 100 Angstroms. The term glass is usually used to indicate that in addition to exhibiting only short range order by X-ray, the material is transparent and exhibits a glass transition before transforming exothermally to a crystalline phase. The term amorphous is sometimes used interchangeably with noncrystalline, and vitreous is synonymous with glassy.

Oxide Systems

Single Oxides

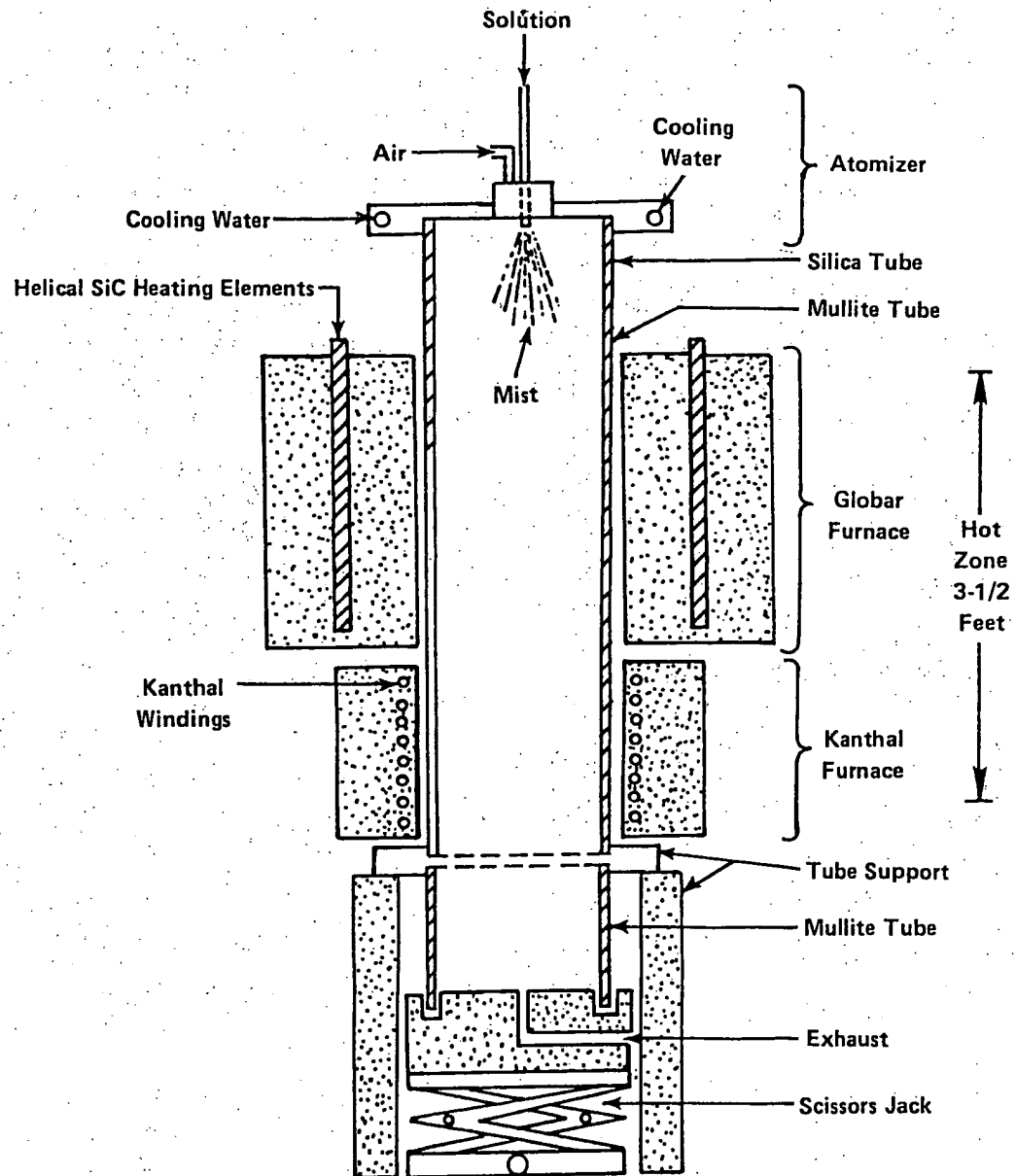Table A-1 summarizes data on single oxides which have been subjected to rapid solidification techniques. Only a few of these oxides were quenched to noncrystalline form. However, it should be noted that many of the experiments utilized estimated quench rates of $<10^6$ K/sec.

Three of the studies included in Table A-1 justify special attention. Suzuki was able to produce noncrystalline Bi_2O_3 as discontinuous film about 0.2 by 0.4 in. (5 by 10 mm) by 20 to 50 μm thick using the roller-plate technique. This suggests that with adequate process development Bi_2O_3 might be produced as a continuous noncrystalline foil. Similarly, Suzuki centrifugally cast ribbons about 0.08 in. (2 mm) wide by up to 4 in. (10 cm) long and 1 to 40 μm thick of mostly amorphous (noncrystalline) V_2O_5. The EDS process (although not a true RS technique) was successfully used by Roy to produce amorphous Al_2O_3 powder.

In summary, several single oxides have been prepared in noncrystalline form, and it is plausible to expect that, with improved RS processing to achieve $>10^6$ K/sec quench rates, many other single oxides will be produced in noncrystalline form.

Binary Oxides

Table A-2 summarizes reported RS experiments on binary oxide systems. These studies have been extensive in number and, in general, were conducted with better controlled and higher quench rates (many estimated at $\geq 10^6$ K/sec) than was true for the single oxide studies. Most of these binary oxide systems yielded quenched noncrystalline or glass products for at least a portion of the compositional ranges explored. The usual quench product was a small flake or splat, sufficient in size for X-ray, DTA, and electrical measurements. The experiments summarized in Table A-2 clearly demonstrate that there is a very wide spectrum of ceramic compositions capable of forming noncrystalline products when solidified at rates $\geq 10^6$ K/sec.

Ternary and More Complex Oxides

Table A-3 summarizes the limited data on reported RS experiments with ternary or more complex oxide systems. The first three table entries are borate (B_2O_3-base) compositions. Since B_2O_3 is a glass former in the traditional sense, it is not surprising that glassy RS products were produced. However, the reason for utilizing RS techniques in these studies was to extend the glass forming range and minimize the chances for any crystalline phases in the quenched glass product. The niobate and tantalate compositions illustrate that glasses can be formed by RS from compositions which are not glass formers by conventional processing. Even the relatively low cooling rate (about 10^4 K/sec) of the laser spin melt and free fall technique produced partially glassy products for the lanthanate-aluminate-gallinate compositions.

Non-Oxide Systems

As indicated by Table A-4 very few non-oxide ceramics have been reported in rapid solidification studies. In the sulfate system RS greatly extended the glass forming capability over conventional (slow) air or water quenching. RS processing also extended the glass forming compositional range for the fluoride system. The crystal compound As_2Te_2 was also produced in amorphous form.

UNIQUE OR POTENTIALLY VALUABLE PROPERTIES OF RS CERAMICS

The application of rapid solidification technology indirectly or directly to ceramic materials can lead to products with unique or high performance properties. An example of indirect utilization is the patent by Shirk[45] on rapid solidification of a glass which is then nucleated and crystallized to yield barium ferrite exhibiting the highest known reported intrinsic coercive force (5,350 Oe). An example of direct RS utilization is the patent by Glass et al.[33] on the RS formation of amorphous niobates and tantalates exhibiting very high values of dielectric constants and ionic conductivity. Glass et al.[33] has reported room temperature ionic conductivity values for amorphous $LiNbO_3$ 10^{20} times larger than extrapolated room temperature values for single crystal $LiNbO_3$.

Table 1 summarizes reported RS ceramics which have exhibited especially interesting electrical, magnetic, or optical properties. These observed properties are discussed in more detail in the following subsections.

Ionic Conductivity

Oxides

A large number of quenched alkali oxide compositions have been explored for ionic conductivity including: tantalates, aluminates, niobates, tungstates, molybdates, bismuthates, and galanates.

Glass et al.[33,52] reported relatively high conductivities for quenched glass alkali niobates and tantalates. Figure 19 shows the variation of Li^+ conductivity as a function of temperature and the activation energies for these glasses plus a $Li_7AlSi_6O_{34}$ glass and single crystal $LiNbO_3$ for comparison. It can be seen that RS $LiNbO_3$ and $LiTaO_3$ are both more conductive than the lithium aluminum silicate glass and much more conductive than single crystal $LiNbO_3$. The extrapolated value of conductivity of $LiNbO_3$ single crystal at room temperature is 10^{20} times smaller than that of the glass. The direct current electronic conductivity for all measurements was less than 10^{-11} (ohm-cm)$^{-1}$.

The lithium conduction of rapidly quenched Li_2O-Al_2O_3, Li_2O-Ga_2O_3, and Li_2O-Bi_2O_3 glasses has been reported by Glass[28] and Nassau.[27] Figure 20 shows the conductivities and activation energies for quenched glass compositions in three systems. Figure 21 shows the variation of ionic conductivity as a function of Li_2O content.

The glasses of composition Li_5AlO_4 and Li_5GaO_4 exhibited considerably greater ionic conductivity than their crystalline counterparts at room temperature (behavior similar to the

TABLE 1. PUBLISHED STUDIES ON RAPIDLY SOLIDIFIED CERAMICS EXHIBITING UNIQUE OR POTENTIALLY VALUABLE PROPERTIES

#	Reference Author	Year	Composition	Geometry and Quench Rate of Samples Studied					Measured Properties of Special Interest	Potential Areas of Application
				Shape	Width, mm	Length, mm	Thickness, μm	Approximate Quench Rate, K/sec		
17	Torii	'82	$La_{0.33}NbO_3$	Flake	–	–	100	–	A new simple cubic perovskite structure was produced with cation vacancies distributed on the A-sites and with predominant orientation of (110) and (220) planes associated with the unidirectional solidification of the melt.	The orientation effect might be utilized for ferroelectric and electrooptic materials. Random distribution of A-site vacancies by rapid quenching might increase oxide ion mobility in ion conductors such as stabilized ZrO_2 and Bi_2O_3.
36	Tatsumisago	'82	$R_2O\text{-}WO_3$ (R=Li, Na, K)	Flake	–	–	–	10^9	Electrochromism was observed for Li and Na containing glasses, the required electric field for coloration (2×10^3 $V\text{-}cm^{-1}$) is lower by an order of magnitude than that reported for amorphous WO_3 films. The $30Li_2O\text{-}70WO_3$ glass exhibited conductivity of 10^{-4} $(\Omega\text{-}cm)^{-1}$.	Electrolytic cells, electrochromic devices.
37	Glass	'77	$Pb_5Ge_3O_{11}$	Flake	5	10	10-20	10^5	$Pb_5Ge_3O_{11}$ glass was utilized to study the evolution of pyroelectric and ferroelectric properties as the ferroelectric phase was crystallized from the glass in a controlled manner. Fine-grained material with dimensions ~10 nm showed very diffuse transition and polarization relaxation, whereas large-grained material (>1μm) exhibited normal ferroelectric behavior.	Pyroelectric applications.
7	Suzuki	'83	$Bi_2O_3\text{-}MoO_3$	Film	~0.5	20	15	–	High temperature fcc form of Bi_2O_3 was produced with grain elongation perpendicular to quench surface coinciding with <111> direction. Electrical conductivity thru the film was 10^3> than along the film.	Devices requiring anisotropic properties.

TABLE 1. (Continued)

#	Reference Author	Year	Composition	Shape	Width, mm	Length, mm	Thickness, μm	Approximate Quench Rate, K/sec	Measured Properties of Special Interest	Potential Areas of Application
18	Roy	'80	Na β-Al_2O_3	Powder	—	—	—	"Equivalent" to 10^6	Amorphous Na β-Al_2O_3 was "stable" after 6 hrs at 1630 C.	Ionic conductors.
35	Nassau	'80	Li_2O-WO_3	Flake	~5	~10	≈10	10^7	Lithium ion conductivities of all of the molybdate and tungstate glasses studied were reasonably high, 10^{-5} - 10^{-6} $(\Omega\text{-cm})^{-1}$ at room temperature. Measured conductivities yielded lithium ion diffusion coefficients about 10^{-11} cm^2/sec in the glass phase and 10^{-16} cm^2/sec in the crystallized material produced by heating the glasses above their crystallization temperatures.	Solid electrolytes or cathodes in lithium batteries. The potential use as cathodes is possible since the glasses can be made electronically conducting by suitable reduction.
27,28	Nassau, Glass	'79,'80	Li_2O-(Al_2O_3, Ga_2O_3, Bi_2O_3)	Flake	3	10	20	10^7	Glasses in all three systems exhibited reasonably high ionic conductivities (up to 10^{-5} $(\Omega\text{-cm})^{-1}$ at room temperature) and low electric conductivities for Li_2O concentrations exceeding 50 mole %. This room temperature conductivity is many orders of magnitude greater than the corresponding crystalline solid.	Solid electrolytes in lithium batteries.
32,33,52	Glass	'77,'78	Li, Na, K Niobates and Tantalates	Flake	~3	~5	≈10	10^7	These glasses exhibited room temperature ionic conductivities as high as 10^{-5} $(\Omega\text{-cm})^{-1}$, electronic conductivities less than 10^{-11} $(\Omega\text{-cm})^{-1}$, and high dielectric constants ranging from 150 at room temperature up to 10^5 at 300 C. Cooling $LiNbO_3$ glass from 670 K in an applied DC field of 100 V/cm, current limited to 10^{-3} A/cm^2, turned the glass black, electrochromism, and exhibited quite a strong dynamic pyroelectric effect and rather non-uniform birefringence. A pyroelectric coefficient of 4×10^{-10} cm^2K was indicated.	Electrolytic cells, capacitors, or dielectric bolometers for measuring temperature (or temperature altering phenomena). Their high polarizability might make them useful in energy storage pyroelectric devices.
41	Gyorgy	'79	$Y_3F_5O_{12}$	Platelets	10	20	15	10^7	Magnetic susceptibility measurements of $Y_3F_5O_{12}$ glass indicate that it is antiferromagnetic with a N'eel temperature of approximately 40 K.	—

TABLE.1. (Continued)

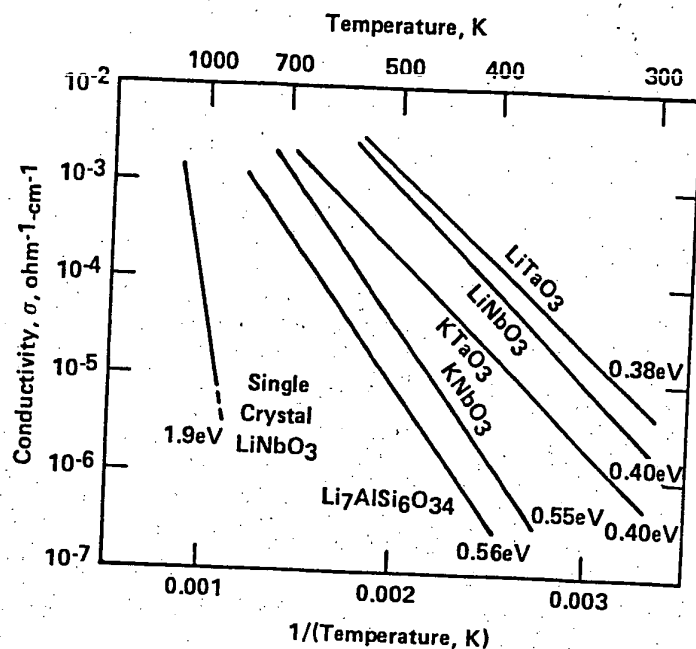| #	Reference		Composition	Geometry and Quench Rate of Samples Studied					Measured Properties of Special Interest	Potential Areas of Application
	Author	Year		Shape	Width, mm	Length, mm	Thickness, μm	Approximate Quench Rate, K/sec		
45,46	Shirk	'71, '72	$BaO \cdot B_2O_3 \cdot Fe_2O_3$ $SrO \cdot B_2O_3 \cdot Fe_2O_3$	Ribbon	—	—	100	—	Barium ferrite or strontium ferrite was produced from the parent glass to yield high performance magnetic properties. Strontium ferrite was produced with an intrinsic coercive force (Hci) = 5800 Oe, a value about 85% of the theoretical Stoner-Wohlfarth Hci for strontium ferrite.	Hard magnetic materials.
47	Laville	'80	$BaO \cdot B_2O_3 \cdot Fe_2O_3$	Ribbon	—	—	50	$\approx 10^6 \cdot 10^8$	Magnetic measurements of the glass showed probable mictomagnetic behavior at low temperature with a maximum magnetic susceptibility at 12(±1) K. At higher temperature, the susceptibility obeyed a Curie-Weiss law with negative Weiss constant and low Curie constant per Fe^{+3} ions. After crystallization, the product was ferrimagnetic.	Magnetic applications.
8,50	Shibata, Kanamori	'80	$PbF_2 \cdot AlF_3$	Ribbon	1	—	10-20	$5 \cdot 10^5$	Absorption spectra measured in the 0.2 to 30 μm wavelength region indicated an infrared absorption edge at around 18 μm from the AlF_3 band. Extrapolation of absorption losses vs. photon energy indicated that the transmission loss minimum (less than 0.1 dB/Km) for $PbF_2 \cdot AlF_3$ should exist in the 3-4 μm wavelength region.	Infrared transmitting optical fibers.

FIGURE 19. TEMPERATURE DEPENDENCE OF THE IONIC CONDUCTIVITY OF ROLLER-QUENCHED ALKALI NIOBATES AND TANTALATES(33,52)

A lithium aluminosilicate glass composition and LiNbO3 single-crystal data are shown for comparison.

previously discussed alkali niobate and tantalate glasses). Crystalline Li_5AlO_4 and Li_5GaO_4 reportedly have conductivities extrapolated to room temperature of $\sigma = 10^{-14}$ $(ohm-cm)^{-1}$ and 3×10^{-12} $(ohm-cm)^{-1}$ and activation energies E_a of about 1.6 and 1.1 eV, respectively, as compared to $\sigma \sim 5 \times 10^{-7}$ $(ohm-cm)^{-1}$ and $E_a \sim 0.5$ eV for the glassy or noncrystalline solids.

A surprising finding was that the ionic radius of the immobile Al^{+3}, Ga^{+3}, or Bi^{+3} cations making up the skeleton or network structure of the glasses has no major effect on the ionic conductivity of the glass (for the Li cation ratio, $X \geq 0.7$ where valid comparisons could be made). This independence of conductivity on the immobile cation radius is in contrast with crystalline materials having the rutile structure in which conductivity increases with increasing radius of the cations comprising the skeletal structure due to the expansion of the lattice.

In three component glasses containing equal mole percentages of both of the binary glasses with X = 0.7, the conductivity is somewhat higher than in either of the two binary glass systems. For example, the $Li_{14}Bi_3Al_3O_{16}$ mixture exhibits considerably higher conductivity than either $Li_7Bi_3O_8$ or $Li_7Al_3O_8$ glasses.

a. $Li_2O\text{-}Al_2O_3$ Glasses

b. $Li_2O\text{-}Ga_2O_3$ Glasses

c. $Li_2O\text{-}Bi_2O_3$ Glasses

FIGURE 20. CONDUCTIVITIES AND ACTIVATION ENERGIES FOR QUENCHED GLASS
COMPOSITIONS IN THREE SYSTEMS[28]

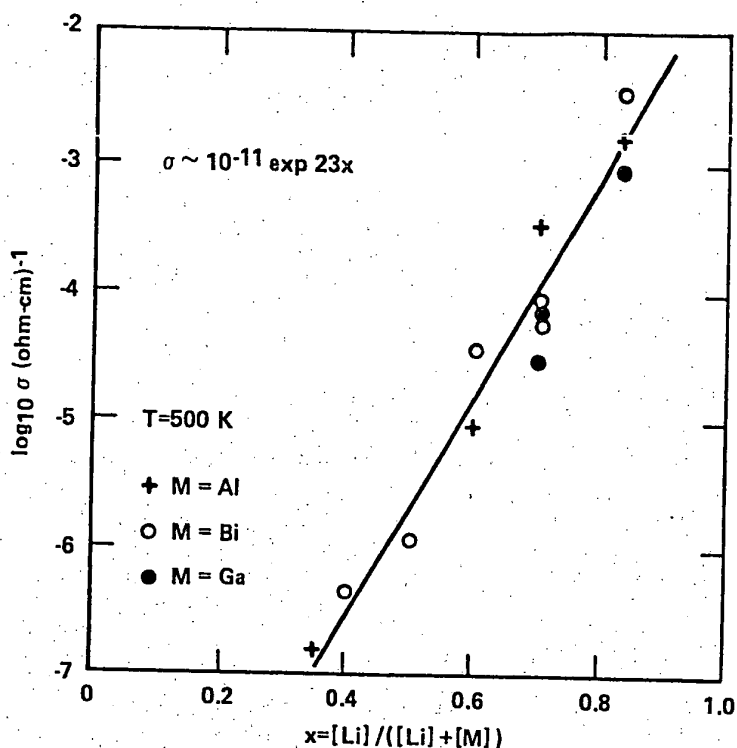FIGURE 21. VARIATION OF THE IONIC CONDUCTIVITY OF Li_2O-M_2O_3 GLASSES (M=Al, Ga, Bi) AS A FUNCTION OF Li_2O CONTENT[28]

Ionic conductivity of quenched alkali tungstate and molybdate glasses was reported by Nassau et al.[35] Lithium ion conductivities of all of the glasses studied were reasonably high, falling in the 10^{-5} to 10^{-6} (ohm-cm)$^{-1}$ range at room temperature, much higher than the polycrystalline phases after crystallization. The measured conductivities yield lithium ion diffusion coefficients about 10^{-11} cm^2/sec in the glass phase and 10^{-16} cm^2/sec in the crystallized material.

Since the Li_2O-WO_3 and Li_2O-MoO_3 glasses can be made electronically conducting by suitable reduction, these materials might be considered for cathodes in lithium batteries.

Sulfates

In a continuing search for high ion conducting quenched glasses, Nassau and Glass[51] explored glasses containing lanthanum and other trivalent sulfates. A wide glass forming region was observed in the Li_2SO_4-$La_2(SO_4)_3$ system with essentially pure glass produced by roller quenching compositions containing 20 to 90 percent lithium. Figure 22 shows the ionic

FIGURE 22. THE IONIC CONDUCTIVITY OF LITHIUM LANTHANUM SULFATE GLASSES AS A FUNCTION OF THE RECIPROCAL TEMPERATURE[51]

conductivity of lithium lanthanum sulfate glasses as a function of temperature for a range of compositions. The relatively high conductivities are of similar magnitude to the quenched oxide glasses produced by these researchers and discussed previously.

Figure 23 presents the observed conductivity of these sulfate glasses as a function of composition at 500 K. The indicated exponential increase of conductivity with lithium ion content is analogous to that observed in the oxide systems: $Li_2O-Al_2O_3$, $Li_2O-Ga_2O_3$, and $Li_2O-Bi_2O_3$. The difference between the sulfate system and oxide systems is that the
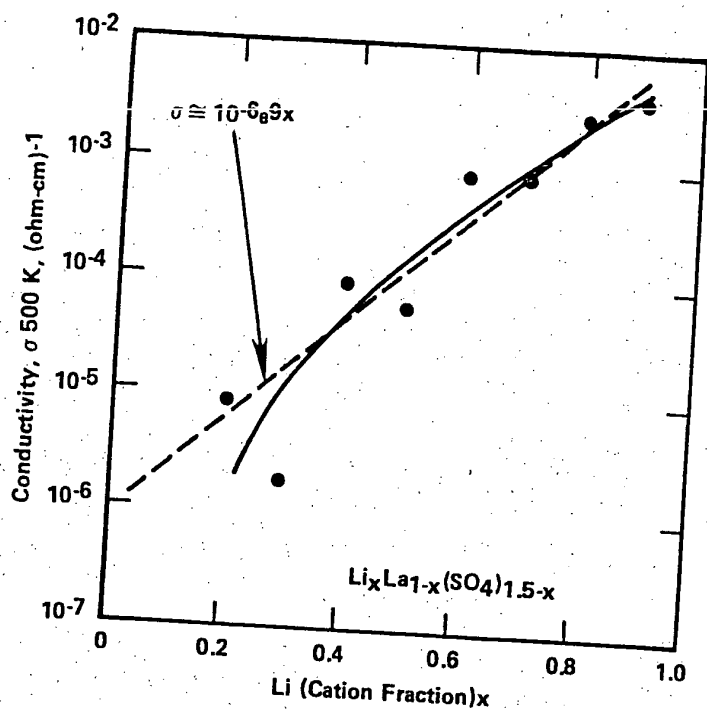
FIGURE 23. THE IONIC CONDUCTIVITY OF LITHIUM LANTHANUM SULFATE GLASSES AS A FUNCTION OF COMPOSITION AT 500 K(51)

exponent is smaller in the sulfates by more than a factor of 2. The absolute conductivity of the sulfate is about the same as that of the oxide; this implies that the mobility is lower in the sulfate glasses.

General Comments

A number of general observations may be extracted from the published studies on ion conductivity of rapidly quenched glasses. Of the noncrystalline materials studied to date, most have exhibited appreciably higher conductivities than the corresponding polycrystalline modification of the same compositions. The isotropic conductivity of a glass may have certain advantages for practical applications in that grain boundary effects associated with the polycrystalline materials are minimized or avoided. This could be particularly important in thin film configurations. Furthermore, the increased disorder of the glass structure which frequently results in an increased ionic mobility also results in a decreased electronic mobility due to decreased overlap of the electronic states of neighboring ions), and hence, an increased ionic transference number. It may also be noted that a high alkali ion mobility in the glass

phase is not necessarily associated with a high crystalline conductivity, so compositions not previously considered for such applications might be worth exploring.

Although relatively high ionic conductivities have been demonstrated for rapidly quenched oxide and sulfate compositions, their values are considerably below the best polycrystalline ceramics such as β-Al_2O_3 [the conductivity of K β"-alumina at 77 F (25 C) is on the order of 10^{-1} (ohm-cm)$^{-1}$]. However, for applications in solid-state batteries, the important properties are electrolyte resistance (not resistivity), the intimacy of contact of the electrodes and electrolytes, and the chemical durability of the electrolyte. If the glasses can be prepared in thin film form directly onto a battery cathode, significantly reduced ionic conductivity might be tolerated.

Glasses Exhibiting Ferroelectric and Pyroelectric Behavior

Glass[32,37] and co-workers at Bell Labs have reported ferroelectric behavior in a number of glass compositions prepared by rapid solidification. Typical temperature dependent, low frequency (1 kHz) dielectric measurements reported by these investigators on lithium niobate and lithium tantalate glasses are shown in Figures 24 and 25, respectively. Upon heating, these glasses crystallized over a relatively narrow temperature range near 770 K in $LiNbO_3$ and 900 K in $LiTaO_3$ to form opaque polycrystalline $LiNbO_3$ and $LiTaO_3$. After crystallization, ε decreased to a much smaller value and remained small upon cooling indicating that the unusual dielectric observations are characteristic only of the glass phase.

Both $LiNbO_3$ and $LiTaO_3$ glasses exhibited a high asymptotic value of $\varepsilon \sim 25$ at low temperature (5 K) which was suggestive of strong dipolar interactions in the glass; ε began to increase at about 40 K and reached a value of about 60 at room temperature. The high ($> 10^5$) and dispersive values of the dielectric measurements are characteristic of disordered ferroelectrics with diffuse phase transitions.

After cooling the $LiNbO_3$ glass from 670 K in an applied direct current field of 100 V/cm, current limited to 10^{-3} A/cm^2, the material turned black (electrochromism) and showed quite a strong dynamic pyroelectric effect and rather non-uniform birefringence. Calibration of the pyroelectric response against single crystal $LiNbO_3$ of similar geometry indicated a pyroelectric coefficient of 4 x 10^{-10} C/cm^2 K. Heating this material to 500 K removed the black coloration but the pyroelectricity remained. Only after heating the glass above 670 K did the pyroelectricity completely disappear.

While these observations are consistent with ferroelectric behavior, the authors[32] note that they are not conclusive since reversible pyroelectricity may be expected from an electret in which ionic charges or dipoles are frozen into nonequilibrium positions after cooling in a
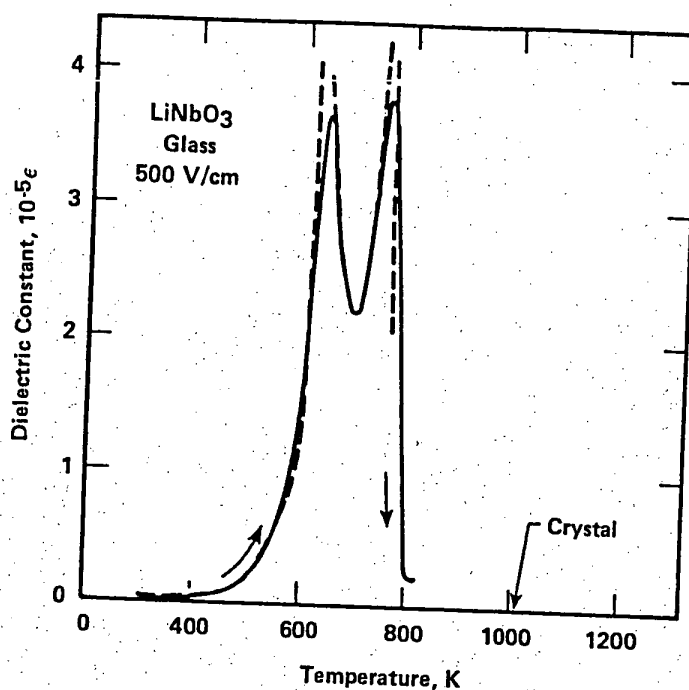
FIGURE 24. TEMPERATURE DEPENDENCE OF THE DIELECTRIC CONSTANT UPON FIRST HEATING OF A VITREOUS LiNbO3 WAFER 0.002 CM THICK MEASURED WITH A FIELD OF 500 V/CM RMS AT 1 kHz(32,37)

field. The experimental observations led them to conclude that more than one microscopic mechanism is necessary to account fully for the dielectric behavior of these glasses. Glass et al. suggest that the high polarizability of these glasses may be useful for applications such as electrostatic energy storage or pyroelectric devices.

Semiconductivity

Vanadium pentoxide, V_2O_5, is a nonstoichiometric oxide containing oxygen vacancies associated with V^{+4} ions. Both crystalline and "noncrystalline" forms of V_2O_5 exhibit semiconductivity behavior arising from the hopping of unpaired electrons between V^{+4} and V^{+5} ions.

Some previous studies of "noncrystalline" V_2O_5 have utilized material prepared by adding glass formers such as P_2O_5 (pure V_2O_5 glass cannot be formed by conventional glass processing).

Livage and Collongues[23] have reported the semiconducting properties of pure V_2O_5 glass prepared by splat cooling. [The ability to form glass V_2O_5 by rapid solidification has also
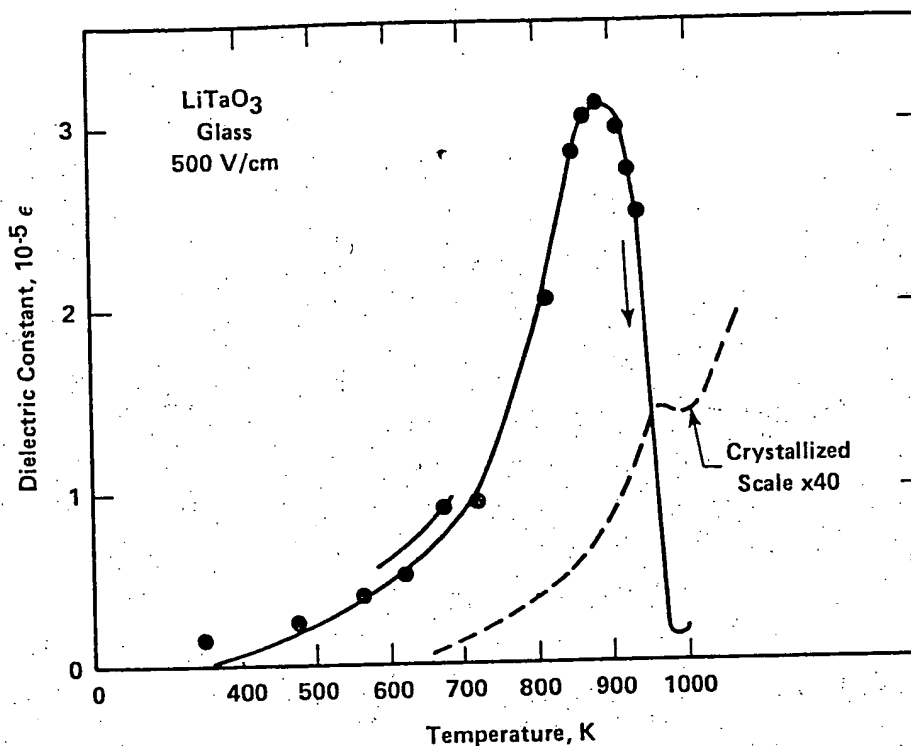
FIGURE 25. TEMPERATURE DEPENDENCE OF THE DIELECTRIC CONSTANT UPON FIRST HEATING OF A VITREOUS LiTaO$_3$ WAFER 0.002 CM THICK MEASURED WITH A FIELD OF 500 V/CM RMS AT 1 kHz[32,37]

been reported by Ohring[6] and Suzuki.[9]] Livage obtained infrared and electron spin resonance spectra for both crystalline and amorphous V$_2$O$_5$. The results indicate that the unpaired 3d electron must be more localized around the vanadium nucleus when the oxide is in the amorphous (glass) form, and the hopping frequency of the electrons is about ten times greater for the crystalline form.

Livage reported that electrical conductivity was about one order of magnitude smaller in the glass than in the crystal. Revcolevschi[53] reports that the conductivity of amorphous V$_2$O$_5$ is about two orders of magnitude lower than that for the crystal.

Livage[54] and Revcolevschi[53] have reported on an interesting fibrous structure for the amorphous V$_2$O$_5$. X-ray and electron diffraction indicate that the fibers presumably correspond to chains of VO$_5$ pyramids directed along the C-axis of the orthorhombic lattice. They are several hundred Angstroms long and about 100 Angstroms in diameter. Presumably this structure accounts for the ready solubility of the amorphous oxide versus the insolubility of crystalline V$_2$O$_5$. No specific applications are apparent for the semiconducting characteristics or unusual microstructure of glassy V$_2$O$_5$.

Magnetic Properties

Gyorgy[41] prepared amorphous (vitreous) $Y_3Fe_5O_{12}$ using the twin roller quenching technique to yield black flakes that could be separated with a small magnet into magnetic and nonmagnetic fractions. Annealing at about 932 F (500 C) in oxygen for several hours produced a deep red color and transparency in the nonmagnetic flakes. The oxygen anneal presumably improved oxygen stoichiometry.

X-ray diffraction of the magnetic flakes showed the diffraction lines of crystalline $Y_3Fe_5O_{12}$ while the nonmagnetic flakes gave weak diffuse scattering with an estimated crystalline contamination of less than 3 percent.

Differential thermal analysis indicated a glass transition at 1022 F (550 C) and a crystallization exotherm at 1364 F (740 C) in the nonmagnetic flakes. After heating these above the crystallization temperature, X-ray diffraction showed only the crystalline $Y_3Fe_5O_{12}$ phase.

Magnetic susceptibility of the amorphous $Y_3Fe_5O_{12}$ was measured as a function of temperature as shown in Figure 26. The χ curve shows a relatively broad peak that may be associated with the Néel temperature at about 40 K. The χ^{-1} curve, analyzed as a simple antiferromagnet, gave a value of θ equal to -500 K and a paramagnetic moment per iron ion of 4.4 μ_B for g = 2.

Fe Mossbauer absorption spectra indicated that the iron is in the Fe^{+3} valence state, and that the iron environment in the amorphous material is different from that in crystalline $Y_3Fe_5O_{12}$ (YIG).

Laville[47] quenched BaO-B_2O_3-Fe_2O_3 glass in the form of short ribbons about 50 µm thick. The product was sorted by means of a 3,000 Oe magnet and only the "nonferromagnetic" product was utilized for measurements. X-ray and electron diffraction indicated that except for a few small crystallites, the selected samples were essentially amorphous.

Differential thermal analysis showed a complex pattern of crystallization starting at 750 K. A complex system of borates crystallizes with changing temperature and $BaFe_{12}O_{19}$ begins to appear at approximately 900 K. Magnetic measurements showed a probable mictomagnetic behavior at low temperature with a maximum of susceptibility at 12 ($\pm$1) K. At higher temperature the susceptibility obeys a Curie-Weiss law with large negative Weiss constant and low Curie constant per Fe^{+3} ions. After crystallization the product is ferrimagnetic and could be used as a permanent magnet. Mossbauer analysis revealed that the glass mainly consists of Fe^{+3} ions in distorted sites and a hyperfine structure at low temperature; the magnetic ordering temperature was estimated to be about 44 ($\pm$1) K.
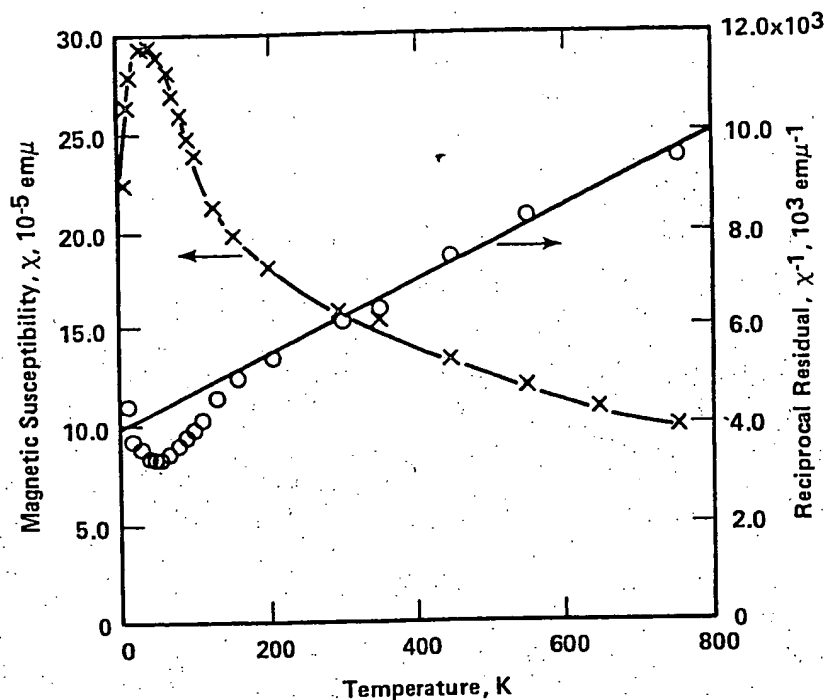
FIGURE 26. χ AND χ^{-1} AS A FUNCTION OF TEMPERATURE FOR AMORPHOUS $Y_3Fe_3O_{12}$[41]

A process patented by Shirk[45,46] employs rapid solidification of a borate composition from which barium or strontium ferrites are then derived by nucleation and crystallization. The process makes it possible to produce nonagglomerated ferrite particles of optimum particle size and magnetic quality without grinding or milling by simply separating the particles from the remaining nonmagnetic phases. The author reports achieving a coercive force of 5,350 Oe for barium ferrite (the highest reported value for this compound).

Optical Properties

Shibata et al.[8] have utilized rapid solidification to widen the glass-forming region of fluorides. They produced quenched glass ribbons (10 to 20 μm thick and 1 mm wide) of PbF_2-AlF_3 (for 30 to 60 mole percent AlF_3) by directing the melt onto a single steel roller rotating at a surface velocity of 15 m/sec. Transmission spectra for some of the PbF_2-AlF_3 glasses (15 μm in thickness) are shown in Figure 27. The higher wavelength absorption edge originates from the AlF_3 absorption band around 18 μm.

By extrapolation of data on absorption losses versus photon energy for PbF_2-AlF_3 samples, it is predicted that minimum loss (less than 0.1 db/km) should exist in the 3 to 4 μm wavelength region. The glasses are resistant to moisture and of low toxicity, but have

FIGURE 27. INFRARED ABSORPTION SPECTRA FOR SAMPLES PREPARED BY ROLLER QUENCHING(8)

high thermal expansion coefficients (13 to 16 x 10^{-6}) and low crystallization temperature [536-626 F (280 to 330 C)]. The overall property data suggest that the PbF_2-AlF_3 glasses have potential as infrared transmitting optical fibers.

Property/Structure Anisotropy

Studies by Torii(17) and Suzuki(7) have demonstrated rapidly solidified ceramics with preferred microstructural orientations. In the study reported by Torii, $La_{0.33}NbO_3$ was rapidly quenched to produce a new cubic perovskite structure instead of orthorhombic. In addition, the quenched structure exhibited predominant orientation of (110) and (220) planes

relative to the quench surface. An additional effect of the rapid quench was to disorder A-site vacancies. The author suggests that the rapid quenching orientational effects might be advantageously applied to ferroelectric or electrooptic materials, and that randomizing of vacancy sites might increase the mobility of ions in ion conductors such as stabilized ZrO_2 or Bi_2O_3.

Suzuki[7] reported producing the high temperature fcc form of Bi_2O_3 with a high degree of orientation by rapid quenching. The high temperature form could be retained within the compositional range of 4 to 6 mole percent of MoO_3 additive. Single roller quenching produced crack-free films with grain elongation (perpendicular to the quench surface) coinciding with the <111> direction.

The electrical conductivity of the film exhibited a high degree of anisotropy as shown in Figure 28. The conductivities along the film length and width were close to 10^{-2} $(ohm-cm)^{-1}$ around 752 F (400 C), three orders of magnitude greater than that along the film thickness. The quenched film became unstable above 842 F (450 C).

Pendant drop extraction experiments at Battelle-Columbus (unpublished data) have produced a variety of quenched forms from high alumina-zirconia melts. By varying process parameters it was possible to form micro-foils, fibers, or spherical particles as illustrated in Figures 29, 30, and 31, respectively. Micro-foils were produced in sizes up to about 1/32 in. wide by 1/4 in. long, discontinuous fibers ranged up to ~1 in. in length, and the particle diameters ranged from about 10 mils down to a few mils. The surface structure of the particles exhibited dendritic crystal growth oriented perpendicular to the surface. Figure 31 shows that these particles have a high surface area, suggesting possible application as catalyst supports. Very fine dendritic structures of particles or fibers might be utilized to form consolidated or composite structures with unique mechanical properties.

Summary of RS Ceramic Properties and Applications

The following summary is based on the preceding discussions and Table 1.

- Surprisingly high lithium ion conductivities have been demonstrated for quenched oxide and sulfide glasses. However, their use in solid-state batteries would have to be justified by some combination of additional features such as the ability to be applied in thin film form or chemical durability because their demonstrated conductivities are still well below crystalline conductors such as $\beta-Al_2O_3$.

- The observed temperature dependence of dielectric constants might be utilized in dielectric bolometers for measuring temperatures or for studying other temperature altering phenomena.

- The high polarizability of some of the glasses might make them useful in electrostatic energy storage or pyroelectric devices.

FIGURE 28. THE TEMPERATURE DEPENDENCE OF DIRECTIONAL DIFFERENCES IN CONDUCTIVITY OF THE QUENCHED FILM, PLOTTED AS LOG σ AGAINST 1000/T, MEASURED AT 1 kHz IN AIR(7)

- A quenched glass precursor used to nucleate and crystallize an optimum crystalline product may have broader applications than that demonstrated by Shirk to produce high performance ferrites.

- The ability to extend glass-forming compositions or produce glasses from new compositions (such as the fluorides) may lead to new high performance optical fibers or other optical devices.

- The ability to produce quenched structures exhibiting new metastable crystalline forms, high order of anisotropy, and randomized vacancy sites may lead to valuable electrical, electrooptic, sensing, or other applications.

K2823-9   ~38X

FIGURE 29. MELT EXTRACTED MICRO-FOILS

In short, a wide variety of interesting property characteristics have been demonstrated for rapidly solidified ceramics. However, in many, if not most potential applications, the utility of such properties depends on being able to form the RS material into a useful configuration, while retaining beneficial properties and without introducing competing side-effects (i.e., scattering loss or lowered dielectric strength in an improved electrooptic).

K2823-1 ~38X

FIGURE 30. MELT EXTRACTED FIBERS

SUMMARY OF THE STATUS OF RAPIDLY SOLIDIFIED CERAMICS TECHNOLOGY

The status of this technology might be characterized as follows:

- Interesting and potentially valuable property characteristics have been demonstrated for RS ceramics in the laboratory—there is no known effort toward commercialization.

- The processing equipment developed produces small flakes, discontinuous foils, or micro-ribbons suitable for laboratory purposes.

- No apparent effort has been expended on how to produce RS ceramics in significant quantities, sizes, and forms for potential commercial use.

In brief, this technology might be characterized as showing tantalizing potential for producing unusual ceramic properties, but development of processing to form RS ceramics in useful configurations while retaining unique properties is needed to permit commercial product development.

31466   a. General Shape of Particles   500X

31467   b. Surface Structure   7500X

FIGURE 31. SEM PHOTOS OF MELT EXTRACTED PARTICLES

THE FUTURE OF RAPID SOLIDIFICATION TECHNOLOGY FOR CERAMICS (RSTC)

The growing number of researchers exploring the properties of rapidly solidified ceramics indicates an emerging awareness of the potential utility of such materials. However, there are several factors which impede the development and application of RS technology to ceramics. These factors include both attitudes and technical difficulties. Research directed toward resolving the technical problems could also moderate negative attitudes.

FACTORS LIMITING THE DEVELOPMENT OF RSTC

Psychological factors which may continue to delay or limit interest in applying rapid solifidication processing to ceramics include:

- Assumption that the low thermal conductivity of ceramics in general makes rapid quenching unfeasible

- Assumption that the thermal fracture susceptibility and brittleness of ceramics implies impracticality of producing shapes and/or sizes of commercial importance

- Assumption that RS is simply a technique for extending the range of glass-forming compositions or solid solutions.

The primary technical factors associated with rapidly solidifying ceramics may be grouped under two categories:

- Factors associated with producing a homogeneous, chemically stable, temperature-controlled melt suitable for delivery to the quench stage (Ceramic materials are in general high melting and include a broad range of chemical reactivities, thus the energy input source for melting and the containment media can be much more demanding than for relatively low melting metals and metal alloys processed in current RS metallurgy.)

- Factors associated with controlling the rapid solidification of the melt effectively.

    For conduction-dominated processes the factors include:

    -- Rapid transport of the melt to the quench surface(s) (high temperature ceramic melts can cool unacceptably by radiation if the transport is too slow)

    -- Spreading or squeezing the melt out into a thin layer in close contact with the quench surface(s). (For many or the majority of ceramic melts, spontaneous wetting of the metal quench surface may not be expected--one solution is to forceably squeeze the melt between two surfaces such as the twin roller or roller-plate techniques and another is to cast the melt into the inside of a spinning drum so that centrifugal force presses the melt against the drum.)

For <u>convection-dominated processes</u> the factors include:

-- Atomization of the melt. [The very high temperatures of ceramic melts pose materials-of-construction problems for atomization equipment. The laser spin melt and free fall cooling studies of Topol[2,22] are the only reported attempts at atomization and quenching of ceramic melts. It seems likely that the reported process was subject to significant variations in the melt temperature and quench rate as indicated by the variation in spherule size and variable glass yields produced.]

PLAUSIBLE PROCESS ROUTES TO COMMERCIAL RS CERAMICS

In order for rapidly solidified ceramics to emerge from the laboratory and achieve commercial relevance, processes must be conceived and demonstrated for producing forms and shapes of commercial utility. Some process routes might be borrowed or modified from development work on rapidly solidified metals. However, RS ceramics are expected to be brittle in contrast to the usual ductility of RS metals. Thus, ceramic forming or consolidation processes must accommodate or circumvent this problem.

The high cooling rates needed to produce glassy or metastable crystalline ceramics limit the dimensions of products that can be directly formed by rapid solidification. In direct forming there must be at least one small dimension through which most of the heat can be rapidly extracted. Forms such as coatings, sheets, or ribbons might be formed directly by RS; but, thick plates, large diameter rods, or bulky three-dimensional shapes would require some form of a secondary consolidation process. Such consolidation would obviously have to be performed under conditions of temperature and time which would not cause transformation of the metastable RS ceramic into equilibrium structures.

Direct Forming

Foils and Ribbons

Some of the RS processes applied to ceramics have produced foil or ribbon-like products. For example, Suzuki[9] centrifugally cast ribbons 1 to 40 µm thick, ~0.08 in. (~2 mm) wide and up to 4 in. (10 cm) long of mostly amorphous V_2O_5. Laville[47] formed small ribbons up to several inches long of $BaO-Fe_2O_3-B_2O_3$ glass by the twin roller technique. Refinement of these or other techniques may make it possible to form continuous foils or ribbons.

Coatings

Plasma spraying is capable of producing coatings containing metastable ceramic phases as illustrated in the work by Wilms,[19] but such coatings are highly heterogeneous in microstructure. Other processes of atomization and impingement might be developed to provide better controlled coatings. Coating processes capable of producing very thin continuous coatings of metastable ceramics could implement applications such as electrodes for lithium batteries.

Indirect Forming

Powders or Flake

The development of processing to produce powder or flake materials in commercial quantities might be the easiest or quickest route to commercial applications. Such "feed" material might then be utilized for consolidation into end products. Although not a true RS process, the EDS process developed by Roy et al.[18] is reportedly capable of ready scale-up to produce a variety of amorphous ceramic powders. Some of the laboratory processes utilized in exploring RS ceramics might be modified and developed to yield powder or flake materials in sufficient quantities for consolidation development.

Consolidation

The consolidation of RS metals is still in the early stages of development, but a recent review of the literature[1] indicates progress. Three approaches have been pursued in efforts to retain the starting RS metal characteristics during consolidation: (1) dynamic compaction, (2) hot forming, and (3) warm consolidation. Success has been reported by researchers in retaining metal glass properties in exploratory applications of all three of the consolidation approaches and a patent has been granted to Morris[55] covering a dynamic compaction process.

There are no known attempts to consolidate rapidly solidified metastable ceramics by any of the three methods noted above for metals. However, there is one reference which indirectly provides hope for consolidating an amorphous ceramic powder without crystallization. Roy[18] has reported the production of amorphous sodium β-Al_2O_3 by the evaporative decomposition of solutions process. This powder retained its noncrystalline character after heating for 6 hours at 2966 F (1630 C). It should be possible to hot

isostatically press (HIP) such a powder to essentially theoretical density at several hundred degrees C below this temperature. Therefore, it is anticipated that the powder should be capable of full consolidation while retaining its amorphous character.

RESEARCH RECOMMENDATIONS FOR ACCELERATING THE DEVELOPMENT OF RAPID SOLIDIFICATION TECHNOLOGY FOR CERAMICS

If the development of rapidly solidified ceramics is allowed to proceed in a manner analogous to that which has occurred for metals, the growth scenario may be as follows:

(1) Continuing exploratory studies of new material systems and obtainable properties will ultimately identify one or more RS material(s) which promise sufficient economic payoff to justify scale-up and production.

(2) As commercial successes are achieved via (1), interest and belief in the potential of RS ceramics will be reinforced and research will expand leading to increasing numbers of special RS materials and associated process commercialization efforts.

Initially, (1) and (2) will lead to a variety of specialized RS processes applicable to limited ceramic compositions, but ultimately RS processing and equipment will be developed which is applicable to a wide range of ceramic materials and product forms.

It is suggested that rapid solidification technology for ceramics would advance more quickly and a broad range of RS ceramics would reach commercialization sooner if the following research/development scenario were pursued:

(1) Major research funding to develop RS process/equipment applicable to a broad range of ceramic materials (including atmospheric processing control) for forming:

— noncrystalline, or glassy powders in quantities sufficient for producing and evaluating prototype products

— "continuous" strip, fiber, or other thin shapes

— thin coatings of RS ceramics on shapes of practical utility.

(2) Research directed toward developing techniques/equipment for consolidating quenched RS ceramic powders into shapes of practical utility while retaining the quenched powder characteristics

(3) Research directed toward exploring attainable mechanical properties of RS ceramics. (Unusual mechanical properties may be achievable via RS ceramics with either glassy or unique polycrystalline structures. This is an apparently totally unexplored area of properties which may lead to properties unattainable by other ceramic processing routes. For example, it may be possible to produce polycrystalline microstructures by crystallization of RS glassy structures which exhibit vastly superior mechanical properties compared with conventionally sintered or hot pressed materials with their "property controlling" grain boundary phases. Such materials could have great practical utility if practical shapes and sizes could be produced via powder consolidation.)

The recommended research thrusts and potential "product" applications are illustrated schematically in Figure 32.
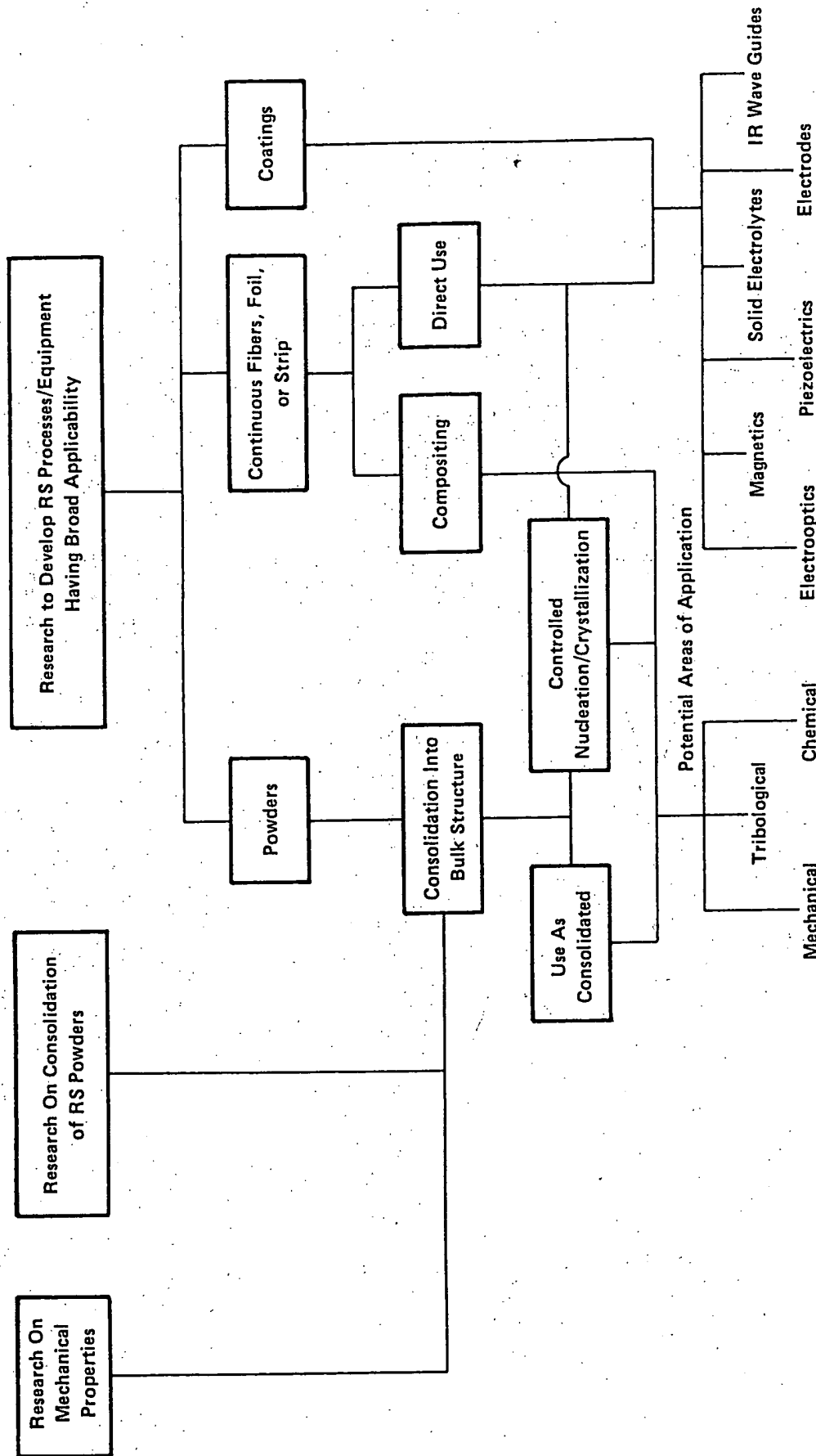
FIGURE 32. SCHEMATIC OF RECOMMENDED RESEARCH AND DEVELOPMENT
ON RS CERAMICS AND POTENTIAL AREAS OF APPLICATION

REFERENCES

(1)   Carbonara, R. S., et al., "State-of-the-Art Review of Rapid Solidification Technology (RST)", Metals and Ceramics Information Center Report, MCIC 81-45 (1981).

(2)   Topol, L. E., et al., "Formation of New Oxide Glasses by Laser Spin Melting and Free Fall Cooling", Journal of Non-Crystalline Solids, 12, 377-390 (1973).

(3)   Pardoe, G.W.F., et al., "Rapid Quenching by the Taylor Wire Technique", Journal of Materials Science, 13, 786-790 (1978).

(4)   Revcolevschi, A., "Techniques for Ultrafast Quenching (Splat Cooling) of Refractory Oxides", High Temperatures - High Pressures, 7, 209-214 (1975).

(5)   Shishido, T., et al., "Ln-M-O Glasses Obtained by Rapid Quenching Using a Laser Beam", Journal of Materials Science, 13, 1006-1014 (1978).

(6)   Ohring, M. and Haldipur, A., "A Versatile Arc Melting Apparatus for Quenching Molten Metals and Ceramics", The Review of Scientific Instruments, 42 (4), 530-531 (April 1971).

(7)   Suzuki, T. and Ukawa, S., "Preparation of a Crack-Free and Grain Oriented Bi_2O_3 Film with fcc Structure", Journal of Materials Science, 18, 1845-1851 (1983).

(8)   Shibata, S., et al., "New Binary PbF_2-AlF_3 Glasses", Materials Research Bulletin, 15 (1), 129-137 (January 1980).

(9)   Suzuki, T., et al., "The Effect of High Pressure on Crystallization of Splat-Cooled V_2O_5", Journal of Non-Crystalline Solids, 24, 355-360 (1977).

(10)   Sarjeant, P. T. and Roy, R., "New Glassy and Polymorphic Oxide Phases Using Rapid Quenching Techniques", Journal of the American Ceramic Society, 50 (10), 500-503 (October 1967).

(11)   Duwez, Pol and Willens, R. H., "Rapid Quenching of Liquid Alloys", Transactions AIME, 227 (2), 362-364 (1963).

(12)   Jantzen, C. M., et al., "Ultra-Rapid Quenching of Laser-Melted Binary and Unary Oxides", Materials Research Bulletin, 15, 1313-1326 (1980).

(13)   Chen, H. S. and Miller, C. E., "A Rapid Quenching Technique for the Preparation of Thin Uniform Films of Amorphous Solids", The Review of Scientific Instruments, 41 (8), 1237-1238 (August 1970).

(14)   Tatsumisago, M., et al., "Rapid Quenching Technique Using Thermal-Image Furnace for Glass Preparation", Journal of the American Ceramic Society, C-97 (July 1981).

(15)   Suzuki, T. and Anthony, A. M., "Rapid Quenching on the Binary Systems of High Temperature Oxides, Materials Research Bulletin, 9, 745-754 (1974).

(16) Nassau, K., et al., "Quenched Metastable Glassy and Crystalline Phases in the System Lithium-Sodium-Potassium Metatantalate", Journal of the American Ceramic Society, 62 (1-2), 74-75 (1979).

(17) Torii, Y., et al., "Crystallization in Rapid Quenching of $La_{0.33}NbO_3$ Melt", Materials Research Bulletin, 17 (6), 727-732 (June 1982).

(18) Roy, D. M., et al., "Innovative Technology for Fabrication of Ceramics: EDS Rapid Solidification Process Application to Specialized Materials", Final Report Bu Mines OFR66-81, 53 (November 1980).

(19) Wilms, V. and Herman, H., "Plasma Spraying of Al_2O_3 and Al_2O_3 - Y_2O_3, Thin Solid Films", 39, 251-262 (1976).

(20) Herman, H., "Properties of Materials Quenched From the Liquid State", Final Report ARO8571.11-MC (1977).

(21) Suzuki, T., et al., "A Roller-Plate Technique for Preparing Uniform Thin Films From the Melt", The Review of Scientific Instruments, 51 (4), 550-551 (April 1980).

(22) Topol, L. E. and Happe, R. A., "Formation of New Lanthanide Oxide Glasses By Laser Spin Melting and Free Fall Cooling", Journal of Non-Crystalline Solids, 15, 116-124 (1974).

(23) Livage, J. and Collongues, R., "Semiconducting Properties of Amorphous V_2O_5 Prepared by Splat Cooling", Materials Science and Engineering, 23, 297-299 (1976).

(24) Morikawa, H., et al., "Glass Forming Ability and Crystallization in the $PbO-Al_2O_3$ System", Journal of Non-Crystalline Solids, 44 (1), 107-112 (May 1981).

(25) Shishido, T., et al., "$Gd_2Al_5O_{12}$ Phase Obtained by Crystallization of Amorphous $Gd_2O_3 \cdot 5/3\ Al_2O_3$", Journal of the American Ceramic Society, 61 (7-8), 373-375 (July-August 1978).

(26) Takamori, T. and Roy, R., "Rapid Crystallization of $SiO_2-Al_2O_3$ Glasses", Journal of the American Ceramic Society, 56 (12), 639-644 (December 1973).

(27) Nassau, K. and Grasso, M., "Quenched Glasses in the Systems of Li_2O With Al_2O_3, Ga_2O_3 and Bi_2O_3", Journal of Non-Crystalline Solids, 34, 425-436 (1979).

(28) Glass, A. M., "Lithium Ion Conduction in Rapidly Quenched $Li_2O-Al_2O_3$, $Li_2O-Ga_2O_3$, and $Li_2O-Bi_2O_3$ Glasses", Journal of Applied Physics, 51 (7), 3756-3761 (July 1980).

(29) Nassau, K., "Rapidly Quenched Glasses", Journal of Non-Crystalline Solids, 42 (1-3), 423-431 (1980).

(30) Monteil, J. B., et al., "Structure Et Mechanisme De Cristallisation Des Produits Obtenus Par Hyper-Trempe Dans Les Systemes $BaO \cdot Fe_2O_3$ et $SrO \cdot Fe_2O_3$", Journal of Solid State Chemistry, 35, 1-8 (1978).

(31) Sarjeant, P. T. and Roy, R., "Ti^{+4} Coordination in Glasses $RO-TiO_2$ System", Journal of the American Ceramic Society, 52 (1), 57-58 (January 1969).

(32) Glass, A. M., et al., "Anomalous Dielectric Behavior and Reversible Pyroelectricity in Roller-Quenched $LiNbO_3$ and $LiTaO_3$ Glass", Applied Physics Letters, 31 (4), 249-251 (August 1977).

(33) Glass, A. M., et al., "Ionic Conductivity of Quenched Alkali Niobate and Tantalate Glasses", Journal of Applied Physics, 49 (9), 4808-4811 (September 1978).

(34) Negran, T. J. and Glass, A. M., "A Study of the Crystallization Kinetics of Roller Quenched $LiNbO_3$ Glass Using Trivalent Chromium Ion Luminescence As a Probe", Physics and Chemistry of Glasses, 20 (6), 140-141 (December 1979).

(35) Nassau, K., et al., "Rapidly Quenched Tungstate and Molybdate Composition Containing Lithium: Glass Formation and Ionic Conductivity", Journal of the Electrochemical Society: Solid-State Science and Technology, 127 (12), 2743-2747 (December 1980).

(36) Tatsumisago, M., et al., "Preparation and Characterization of Rapidly Quenched Glasses in the Systems R_2O-WO_3 (R=Li, Na, K)", Journal of Materials Science, 17, 3593-3597 (1982).

(37) Glass, A. M., et al., "Evolution of Ferroelectricity in Ultrafine-Grained $Pb_5Ge_3O_{11}$ Crystallized From the Glass", Journal of Applied Physics, 48 (12), 5213-5216 (December 1977).

(38) Nassau, K., et al., "The Crystallization of Vitreous and Metastable $Pb_3Ge_3O_{11}$", Journal of Crystal Growth, 42, 574-578 (1977).

(39) Anthony, A. M., et al., "Crystallization and Ordering of Complex Oxide Structures. I. 'Splat-Cooled' $Nb_2O_5-TiO_2$", Journal of Solid State Chemistry, 21, 233-241 (1977).

(40) Takamori, T. and Roy, R., "Metastable Modification of $SrSiO_3$", Journal of the American Ceramic Society, 58 (7-8), 348 (July-August 1975).

(41) Gyorgy, E. M., et al., "The Magnetic Properties of Amorphous $Y_3Fe_5O_{12}$", Journal of Applied Physics, 50 (4), 2883-2886 (April 1979).

(42) Coutures, J. P. and Benezech, G., "Refractory Glasses Based on Aluminum and Neodynium Sesguioxide", Materials Research Bulletin, 10, 539-546 (1975).

(43) Coutures, J. P. and Benezech, G., "Characterization Structural Et Thermigue D'Amorphes A Base D'Alumine Et D'Oxydes De Lanthanides", (Lm=La, Ce, Pv, Nd, Sm, Gd, Tb), Review of Physics Applied, 12, 667-672 (1977).

(44) Revcolevschi, A., "Cooling-Rate Determination in Splat-Cooling of Oxides", Journal of Materials Science Letters, 11, 563-565 (1976).

(45) Shirk, B. T., "Production of Barium Ferrite", U.S. Patent 3,630,667 (December 28, 1971).

(46) Shirk, B. T., "Formation and Magnetic Properties of Strontium Ferrite Crystallized From Glasses in the $B_2O_3-SrO-Fe_2O_3$ System", American Ceramic Society Bulletin, 51 (4), 365-366 (April 1972).

(47) Laville, H. and Bernier, J. C., "Mictomagnetism in a New $BaO \cdot Fe_2O_3 \cdot B_2O_3$ Glass", Journal of Materials Science, 15, 73-81 (1980).

(48) Tatsumisago, M., et al., "Infrared Spectra of Rapidly Quenched Glasses in the Systems $Li_2O-RO-Nb_2O_5$ (R=Ba, Ca, Mg)", Journal of the American Ceramic Society, <u>66</u> (2), 117-119 (February 1983).

(49) Nassau, K., et al., "Quenched Metastable Glassy and Crystalline Phases in the System Lithium-Sodium-Potassium Metaniobate-Tantalate", Journal of the American Ceramic Society, <u>62</u> (9-10), 503-510 (September-October 1979).

(50) Kanamori, T., et al., "Preparation and Properties of PbF_2-AlF_3 Glass", Japan Journal of Applied Physics, <u>19</u> (2), L90-L92 (February 1980).

(51) Nassau, K. and Glass, A. M., "Quenched Glasses Containing Lanthanum and Other Trivalent Sulfates", Journal of Non-Crystalline Solids, <u>44</u>, 97-105 (May 1981).

(52) Glass, A. M., et al., "Amorphous Metal Oxide Material Between Electrodes of a Cell", U.S. Patent 4,130,694 (December 19, 1978).

(53) Revcolevschi, A., "Rapid Solidification of Nonmetals", <u>Treatise on Materials Science and Technology V20</u>, Edited by H. Herman, Academic Press, New York, 73-116 (1981).

(54) Livage, J., et al., "Hydratation Et Texture Fibreuse De V_2O_5 Amorphe", Materials Research Bulletin, <u>13</u> (11), 1117-1124 (1978).

(55) Morris, D. G., "A Method of Producing Large Objects from Rapidly Quenched Non-Equilibrium Powders", European Patent 22,423 (January 1, 1981).